In-plane vibration characterization of microelectromechanical systems using acousto-optic modulated partially incoherent stroboscopic imaging

Dung-An Wang[a], Fang-Wen Sheu[b] and Yen-Sih Chiu[a]

[a]Graduate Institute of Precision Engineering, National Chung Hsing University, Taichung 40227, Taiwan
[b]Department of Electrophysics, National Chiayi University, Chiayi 60004, Taiwan

E-mail: daw@dragon.nchu.edu.tw

Abstract

A technique using acousto-optic modulated partially incoherent stroboscopic imaging for measurement of in-plane motion of microelectromechanical systems (MEMS) is presented. Vibration measurement is allowed by using flashes of the partially incoherent light source to freeze the positions of the microstructure at twelve equally spaced phases of the vibration period. The first-order diffracted beam taken out by an acousto-optic modulator (AOM) from the light beam of a laser is made partially incoherent by a rotating diffuser and then serves as the stroboscopic light source. Both the MEMS excitation signal and the flash control signal are provided by a dual-channel function generator. The main advantage of this measurement method is the absence of a stroboscopic generator and a high speed digital camera. Microscale prototypes are fabricated and tested. Quantitative estimates of the harmonic responses of the prototypes are obtained from the recorded images. The results agree with those obtained with a commercial MEMS motion analyzer[TM] with relative errors less than 2%.

_____

* Corresponding author: Tel.:+886-4-22840531 ext. 365; fax:+886-4-22858362

E-mail address: daw@dragon.nchu.edu.tw (D.-A. Wang).

1. Introduction

Knowledge of the vibration behaviors of MEMS devices operating in the dynamic mode are needed at various stages of their development. Requirement of better product quality and reliability further demands for efficient measurement techniques with ease of use. Various optical methods have been proposed to measure in-plane motion of microstructures, which have the advantages of large field of view, non-contacting and non-contaminating which are critical for characterization of MEMS devices. Among these optical methods, interferometric microscopy [1,2], stroboscopic illumination combined with image processing [3,4], and laser Doppler vibrometer [5] are power techniques for measurement of in-plane motion or vibration amplitude [6].

The microscopic interferometry has been used for measuring small displacements. Yang et al. [7] performed static and dynamic displacement measurement of microstructures using stroboscopic speckle pattern interferometry, where a control system is required to synchronize stroboscopic illumination with vibration signal, and a reference object mounted on a piezoelectric translator is needed to provide phase shifting capability. Zhou and Chau [8] proposed a modified grating interferometer to measure in-plane motion of microstructures with a reflection phase grating beam elements formed on them. Zhong et al. [9] reported a laser Doppler system for in-plane motion measurement of MEMS devices. A signal processing scheme is necessary to demodulate the signal and to

produce a time-resolved voltage proportional to the transient velocity. The velocity of the vibrating structure is extracted using a pulse inserting method and the displacement is calculated by integration. Systems based on stroboscopic illumination and video imaging have been developed for motion measurement of MEMS devices, where displacements are estimated directly from the images of the devices acquired at evenly-spaced phases of the excitation signal. As pointed out by Davis and Freeman [10], the duration of the strobe pulse limits the maximum frequency of motion that these systems can measure, and the image resolution with light microscopy is limited to the wavelength of light. Freeman and Davis [11] applied this technique to measure the frequency response of a microfabricated accelerometer. Hunsinger and Serio [12] combined video imaging and a light-emitting diode (LED) stroboscope to characterize in-plane MEMS motion. A subpixel accuracy using an interpolation and correlation motion estimation algorithm is obtained. A microscope is needed to reach nanometer resolution of their method.

Video microscopy combined with stroboscopic imaging has been gaining attention in MEMS in-plane motion characterization. One advantage of stroboscopic sampling is that the time resolution is determined by the width of the sampling pulse [13]. However, since the MEMS device may operate at a fixed excitation frequency, a phase locking scheme, along with pulse picking, must be used to synchronize the optical sampling pulses to the operating MEMS device. In this paper, a system for in-plane vibration measurement of MEMS devices based on acousto-optic modulated partially incoherent stroboscopic illumination and video imaging is presented. The novelty of this system lies on the implementation of the acousto-optic modulated partially incoherent stroboscopic illumination. Both the MEMS excitation signal and the flash control signal

3

are generated by a dual-channel function generator. The experimental setup of the measurement system is described. Prototypes of microstructures are fabricated using an electroforming process. Experiments are carried out to demonstrate the effectiveness of the system for in-plane vibration measurement.

2. In-plane MEMS vibration measurements principle

2.1 Measurement setup

A schematic of an optical system served to measure in-plane vibration of MEMS is shown in Fig. 1. The substrate with microstructures on it is held by a 3-axis translation stage. The microstructures can be excited electromagnetically by a solenoid. The input sinusoidal AC current of the solenoid is supplied by a function generator (WW5062, Tabor Electronics Ltd., Israel). With an AC current passes through the coil of the solenoid, an in-plane force is induced to drive the microstructure into vibration. A 5 mW (632.8 nm) He-Ne laser (1125P, JDS Uniphase, Singapore) is used as the light source. The first-order diffracted beam is taken out by an AOM (AOM-802A1, IntraAction Co., USA) from the light beam of the laser. A rotating diffuser is used to smoothen the laser intensity profiles and avoid the adverse interference and speckle effects [14,15]. The coherent laser light beam is transformed into a partially incoherent light beam which is composed of many fast fluctuating tiny light spots and can be used to enhance the beam uniformity and improve the imaging quality [15]. The scattered light beam is collimated by a 10X microscope objective lens and then is divided into two parts by a cubic beam splitter. One beam is used to illuminate the microstructure on the substrate through another focusing microscope objective, and the other beam is not used. The reflected

4

light beam from the microstructure passes through the beam splitter again and is directed into a charge-coupled device (CCD) camera (LBP-2-USB, Newport Co., USA) by the same microscope objective which serves now as an imaging lens. The camera has a sensor active area of 6.47 mm x 4.83 mm and a pixel size of 8.6 μm x 8.3 μm. The image taken by the CCD camera is recorded by a frame grabber in a personal computer (PC).

2.2 Stroboscopic illumination device

Vibration measurement is allowed by using flashes of the partially incoherent light source to freeze the positions of the microstructure at twelve equally spaced phases of the vibration period. The laser light is strobed once per MEMS excitation period at a selected phase. For a CCD camera with a relatively low frame rate, each recorded frame may take several flashes, and the photons available for the CCD sensor can be increased. After each frame grabbing of the specified phase, the flash phase is shifted consecutively by $\pi/6$ radians. This process is repeated for the chosen phases. Images of the twelve phases are correspondent to the twelve positions of the microstructure in a period. By manually analyzing the successively taken images, the in-plane vibration amplitude of the microstructure can be obtained based on the twelve positions during one motion period.

The approach to the vibration measurement presented here is similar to the work reported by Serio et al. [16], where a specialized phase shift stroboscopic generator is used to provide all the needed control signals. Dissimilar to their method, the laser light flashes are supplied by the first-order diffracted beam out of an AOM, and both the MEMS excitation signal and the flash control signal are provided by a dual-channel function generator, requiring no need for a stroboscopic generator and a high speed

digital camera. Through the partially incoherent stroboscopic light, relatively high precision of in-plane vibration characterization of the microstructures can be achieved with the presented stroboscopic imaging technique.

As shown in Fig. 2, the continuous sinusoidal signal supplied by a function generator serves the purpose to excite the microstructure. The flash signal with a specified phase and duration is the input to the AOM driver. AOMs can be used for strobing a laser light source [17]. The modulation in an AOM is based on the elasto-optic effect [18-20]. With acoustic waves passing through the crystal of an AOM, there is a grating effect generated in the crystal that diffracts the light at various orders [21]. The AOM is positioned at a particular angle to the laser light beam to maximize the first-order diffraction. When the frequency of the flash signal is close to the frequency of the vibrating microstructure, the in-plane motion can be captured by a standard CCD camera. As shown in Fig. 3, for a particular incidence angle θ_B, only one diffraction order is produced in the Bragg regime, and the others are annihilated by destructive interference. The angle θ_B is defined as [21-23]

$$\theta_B = \sin^{-1}(\frac{\lambda F_A}{2v}) \tag{1}$$

where λ is the incident light wavelength, F_A the acoustic frequency and v the acoustic velocity. For the light source, a 632.8 nm HeNe laser, the AOM, a 80 MHz acoustic frequency and the acousto-optic material crystal, which acoustic velocity is taken as 5500 m/sec, the AOM should be positioned as a Bragg angle, θ_B, of 4.6 mrad based on Eq. (1) in order to optimize the first-order efficiency. When the crystal in the AOM is excited, an acoustic grating is created thereby splitting the laser beam into the zeroth- and first-

6

order Bragg diffractions [21]. The first-order diffraction is used for the measurements. From the resulting images, the periodic motion of the microstructure is determined. Fig. 4 schematically shows the successive positions of the microstructure corresponding to the twelve selected phases of the periodic motion.

3. MEMS device fabrication and testing

3.1 Device description

A microstructure which can be resonated in a lateral direction was selected to demonstrate the motion measurement system. Fig. 5(a) is a schematic of the microstructure. A Cartesian coordinated is also shown in the figure. The structure is a compliant chevron-type mechanism consisting of a shuttle mass, flexible hinges, hinged beams and lateral springs. The flexible hinges facilitate the rotation of the hinged beams. Upon the application of a reciprocating force F in the x direction to the hinged beams, the flexible hinges and lateral springs deflect, and the in-plane motion of the mechanism can be excited while the frequency of the actuating force F is properly selected. The displacement in the y direction is constrained due to the structure geometry and the loading conditions. Fig. 5(b) shows a schematic of a quarter model of the device with its dimensions L_1 μm, L_0 μm, L_s μm, t_1 μm, t_0 μm, t_s μm, and θ indicated in the figure.

3.2 Fabrication

Prototypes of the lateral resonators have been fabricated by a simple electroforming process on glass substrates. Since the resonators are electromagnetically stimulated by a solenoid in the experiments, a cobalt-nickel (Co-Ni) alloy is selected as

the structural layer due to its relatively high saturation magnetization. Fig. 6 shows the fabrication steps, where only two masks are used. First, a 2 μm-thick titanium metallization layer is deposited on the whole glass substrate. Next, a 5 μm-thick photoresist (AZ4620) is coated and patterned on top of the titanium seed layer. Then, the titanium layer is wet-etched and a 0.4 μm-thick copper layer is sputtered to prepare a seed layer for electrodeposition of a copper sacrificial layer. Next, the copper sacrificial layer is electrodeposited using an acid sulfate bath with the chemical compositions listed in Table 1 and patterned by a lift-off process. After a 10 μm-thick photoresist (AZ4620) is coated and patterned, a copper layer is electrodeposited. Then, the photoresist is removed and a 10 μm-thick photoresist (AZ4620) is coated and patterned on top of the copper sacrificial layer to prepare a mold for electrodeposition of a Co-Ni structural layer. Into this mold a Co-Ni layer is electrodeposited using a bath with the chemical compositions listed in Table 2. The thickness of the movable structure is nearly 10 μm. Finally, the photoresist is removed and the copper sacrificial layer is wet etched to release the Co-Ni structural layer. Figs. 7 and 8 show an optical microscope (OM) photo of an array of the fabricated devices, and a close-up view of one device, respectively. Each device in the array is designed with a different first-mode resonance frequency.

3.3 Testing

In order to demonstrate the motion measurement system, the fabricated lateral resonators were electromagnetically stimulated with a solenoid. The experimental apparatus is shown schematically in Fig. 9(a). A 1-mm-diameter copper coil with 300 turns at 1 ohm coil resistance is wound around an iron mandrel with a diameter of 9.4 mm and a length of 10.85 cm. One end of the mandrel is sharpened and bended to

8

facilitate the actuation of the in-plane motion of the resonators as shown in Fig. 9(b). There is a 3 mm wide gap between the end surface of the shuttle mass of the resonator and the tip of the mandrel.

Fig. 10 is a photo of the experimental apparatus and the optical measurement setup. The system is placed on a vibration isolation table to minimize the effects of external vibrations. Measurements are taken with a sinusoidal voltage of 3 V_{pp} and different frequencies applied to the solenoid. The generated magnetic force and the spring-like effect of the microstructure drive the resonator into vibration. Stroboscopic illumination is used to take stop-action images at various phases of periodically driven motions of the resonator under test. Typical images of twelve phases of a resonator are shown in Fig. 11. As expected from the design of the device, motions in the y direction are small compared to the motions in the x direction. Fig. 12 shows the displacements of the resonator corresponding to the twelve stimulus phases. The displacements are estimated by measuring the lateral distance between a point on the moving shuttle and a fixed reference point on the glass substrate. The moving shuttle and the fixed reference point are indicated in Fig. 11(a). Half the peak-to-peak displacement of the curve can be taken as the vibration amplitude of the resonator at the driving frequency.

Harmonic analyses of three selected resonators are carried out over a frequency range of 0.001-4 kHz with the supply sinusoidal voltage. The frequency increment is 100 Hz. Once an interval of possible resonance frequencies is found, the interval is repeatedly bisected until an approximate resonance frequency is determined. To lower the complexity of manual recording and manual analysis for a large number of images,

we choose only several representative points of frequency around the resonance frequency to measure the vibration amplitude. The dimensions of the three resonators A, B, and C are listed in Table 3. Quantitative estimates of vibration amplitudes at different driving frequencies are obtained from the recorded images. Figs. 13, 14 and 15 show the in-plane vibration amplitude as a function of the driving frequency for the resonators A, B, and C, respectively. The first-mode resonance frequencies were detected at 3080 Hz, 1689 Hz, and 1872 Hz for the resonators A, B, and C, respectively. In order to prove the effectiveness of the presented technique, a commercial MEMS motion analyzer™ (MMA G2, Umech Technologies, USA) is used to obtain the harmonic responses of the three resonators. The MMA G2 can measure the three-dimensional motion of microstructures with subnanometer resolution. The results obtained with the MEMS motion analyzer for the resonators A, B, and C are also shown in Figs. 13, 14 and 15, respectively, and the first-mode resonance frequencies are determined as 3112 Hz, 1671 Hz, and 1833 Hz for the resonators A, B, and C, respectively. The results obtained with the presented technique are comparable to those obtained with the MEMS motion analyzer with relative errors of 1%, 1%, and 2% for the resonators A, B, and C, respectively. Thus, relatively high precision of in-plane vibration characterization of the microstructures may be achieved with the presented acousto-optic modulated partially incoherent stroboscopic imaging technique.

4. Discussions

The frequency range of the proposed measurement technique is limited by the maximum frequency of the stroboscopic lighting. In the experimental setup, both the MEMS excitation signal and the flash control signal are provided by the commercial

dual-channel function generator. The frequency of the pulse provided by the function generator used in this investigation can be as high as 7.5 MHz, which sets the upper limit of vibration frequency measurement of the microstructures. The frequency range can be increased by using a function generator capable of supplying higher pulse frequencies.

The measurement setup used in this investigation has a displacement resolution of about 0.01 μm, which is determined by the CCD pixel size and the magnification ratio of the imaging system. For measuring smaller vibration amplitudes, the CCD camera can be placed far away from an imaging microscope objective lens. A higher resolution can also be obtained using a higher magnification for the microscope objective. For the requirement of a much higher displacement resolution, the technique of image subtraction [7] at various phases could be applied under the help of the partially incoherent light illumination of the measurement system. When a large field of view is required in order to measure mode shapes of the device, the CCD camera can be mounted on a macro-zoom lens. The proposed technique has an acceptable lateral resolution of in-plane motion in the initial testing stage of the device development and a relative ease of operation.

5. Conclusions

A new technique to measure in-plane motion of microstructures by acousto-optic modulated partially incoherent stroboscopic imaging is presented. An AOM is used for strobing a laser light source. The laser light flashes are supplied by the first-order diffracted beam out of the AOM, and both the microstructures' excitation signal and the flash control signal are provided by a dual-channel function generator, requiring no need for a stroboscopic generator and a high speed digital camera. To depress the image

11

speckle noise induced by the high coherence laser light, we use a rotating diffuser to transform the laser light flashes to a partially incoherent stroboscopic light source, obtaining a spatially homogeneous illumination. Using the images of the successive positions of the microstructure corresponding to the twelve selected phases of the periodic motion, the harmonic response and mode shapes of the microstructures can be determined.

In order to confirm the effectiveness of the motion measurement system, prototypes of microstructures are fabricated on glass substrates using a simple electroforming process. The fabricated lateral resonators are electromagnetically stimulated with a solenoid. Quantitative estimates of the harmonic responses of the resonators are obtained from the recorded images. The results obtained with the presented technique are comparable to those obtained with a commercial MEMS motion analyzer^{TM} with relative errors less than 2% for the resonators under test. The presented acousto-optic modulated partially incoherent stroboscopic imaging technique provides a simple and efficient means for in-plane vibration characterization of microstructures. Due to the absence of a stroboscopic generator and a high speed digital camera, this vibration measurement system may be inexpensive and can be easily integrated into research and fabrication facilities.

Acknowledgement

References

[1]   W Hemmers, M.S. Mermelstein, D.M. Freeman, Nanometer resolution of three-dimensional motions using video interference microscopy, Proceedings of the 12th IEEE MEMS'99, Orlando, Florida, August 1999, pp. 302-308.

[2]   D.J. Burns, H.F. Helbig, A system for automatic electrical and optical characterization of Microelectromechanical devices, Journal of Microelectromechanical Systems 8 (1999) 473-482.

[3]   A. Hafiane, S. Petrigrand, O. Gigan, S. Bouchafa, A. Bosseboeuf, Study of sub-pixel image processing algorithms for MEMS in-plane vibration measurements by stroboscopic microscopy, Proceedings of SPIE, Vol. 5145, 169; doi:10.1117/12.500141, 2003.

[4]   S. Petitgrand, A. Bosseboeuf, Simultaneous mapping of out-of-plane and in-plane vibrations of MEMS with (sub)nanometer resolution, Journal of Micromechanics and Microengineering 14 (2004) S97-S101.

[5]   G. Rinaldi, M. Packirisamy, I. Stiharu I, Dynamic testing of micromechanical structures under thermo-electro-mechanical influences, Measurement 40 (2007) 563-574.

[6]   A. Bosseboeuf, S. Petitgrand, Characterization of the static and dynamic behaviour of M(O)EMS by optical techniques: status and trends, Journal of Micromechanics and Microengineering 13 (2003) S23-S33.

[7]   L.X. Yang, M. Schuth, D. Thomas, Y.H. Wang, F. Voesing, Stroboscopic digital speckle pattern interferometry for vibration analysis of microsystem, Optics and Lasers in Engineering 47 (2009) 252-258.

[8]   G. Zhou, F. S. Chau F S, Grating-assisted optical microprobing of in-plane and out-of-plane displacements of Microelectromechanical devices, Journal of Microelectromechanical Systems 15 (2006) 388-395.

[9]   Y. Zhong, G. Zhang, C. Leng, T. Zhang, A differential laser Doppler system for one-dimensional in-plane motion measurement of MEMS, Measurement 40 (2007) 623-627.

[10]   C.Q. Davis, D.M. Freeman, Using a light microscope to measure motions with nanometer accuracy, Optical Engineering 37 (1998) 1299-1304.

[11]   D.M. Freeman, C.Q. Davis, Using video microscopy to characterize micromechanical systems, IEEE/LEOS Summer Topical Meetings, 1998, pp. 9-10.

[12]   J.J. Hunsinger, B. Serio, FPGA implementation of a digital sequential phase-shift stroboscope for in-plane vibration measurements with subpixel accuracy, IEEE Transactions on Instrumentation and Measurement 57 (2008) 2005-2011.

[13]   T. Eiles, G. Woods, V. Rao, Optical probing of flip-chip-packaged microprocessors, 2000 IEEE International Solid-State Circuits Conference, Digest of Technical Papers, San Francisco, CA, 2000, pp. 220-221.

[14]   M. Mitchell, Z. Chen, M.-F. Shih, M. Segev, Self-trapping of partially spatially incoherent Light, Phys. Rev. Lett. **77** (1996) 490-493.

[15]   F.-W. Sheu, J.-Y. Chen, Fiber cross-sectional imaging by manually controlled low coherence light sources, Opt. Express 16 (2008) 22113-22118.

[16]   B. Serio, J.J. Husinger, B. Cretin, In-plane measurements of Microelectromechanical systems vibrations with nanometer resolution using the correlation of synchronous images, Review of Scientific Instruments 75 (2004)

3335-3341.

[17] S. Hisada, T. Suzuki, S. Nakahara, T. Fujita, Visualization and measurements of sound pressure distribution of ultrasonic wave by stroboscopic real-time holographic interferometry, Japanese Journal of Applied Physics 41 (2002) 3316-3324.

[18] A.A. Maradudin, E. Burstein, Relation between photoelasticity, electrostriction, and first-order Raman effect in crystals of the diamond structure, Physical Review 164 (1967) 1081-1099.

[19] L. Jodlowski, Optimisation of construction of two-channel acousto-optic modulator for radio-signal phase detection, Opto-Electronics Review 11 (2003) 55-63.

[20] A.F. El-Sherif, T.A. King, High-energy, high-brightness Q-switched Tm^{3+}-doped fiber laser using an electro-optic modulator, Optics Communications 218 (2003) 337-344.

[21] M.M. Pai, G. Rinaldi, N. Sivakumar, M. Packirisamy, Low-frequency static characterization of microstructures using acousto-optic modulated stroboscopic interferometer, Optics and Lasers in Engineering 47 (2009) 230-236.

[22] J. Neev, F.V. Kowalski, 1990 Optical frequency scanning without deflection using an acoutooptic modulator, IEEE Journal of Quantum Electronics 26 (1990) 1682-1685.

[23] G. Spirou, I. Yavin, M. Weel, A. Vorozcovs, A. Kumarakrishnan, P.R. Battle, A high-speed-modulated retro-reflector for lasers using an acousto-optic modulator, Canadian Journal of Physics 81 (2003) 625-638.

List of figures

Table 1 Chemical composition and operation conditions for the copper electroplating solution.

Chemical/plating parameter	Amount/value
Copper Sulfate ($CuSO_4 \cdot 5H_2O$)	200 g/L
Sulfuric acid, 96% (H_2SO_4)	75 g/L
Hydrogen chloride (HCl)	0.144 ml /L
Bath temperature	25 °C
Plating current type	dc current
pH of the solution	1
Plating current density	1.5 A/dm^2
Deposition rate	0.3 μm/min
Anode-cathode spacing	105 mm
Anode type	titanium

Table 2 Chemical composition and operation conditions for the Co-Ni electroplating solution.

Chemical/plating parameter	Amount/value
Nickel sulfamate ($CoCl_2 \cdot 6H_2O$)	0.2 mol/L
Boric acid (H_3BO_3)	30 g/L
Nickel chloride ($NiCl_2 \cdot 6H_2O$)	0.9 mol/L
Saccharin	0.7 ml/L
Bath temperature	50 °C
Plating current type	dc current
pH of the solution	4-4.5
Plating current density	0.25 A/dm^2
Deposition rate	0.11 μm/min
Anode-cathode spacing	105 mm
Anode type	titanium

Table 3 Dimensions of the resonators under test. The symbols L_1, L_0, L_s, t_1, t_0, t_s, and θ are indicated in Fig. 5(b).

Device	L_1 (μm)	L_0 (μm)	L_s (μm)	t_1 (μm)	t_0 (μm)	t_s (μm)	θ (degree)
A	600	300	200	5	40	15	2.3
B	300	900	200	7	40	15	2.3
C	300	900	200	8	40	15	2.3
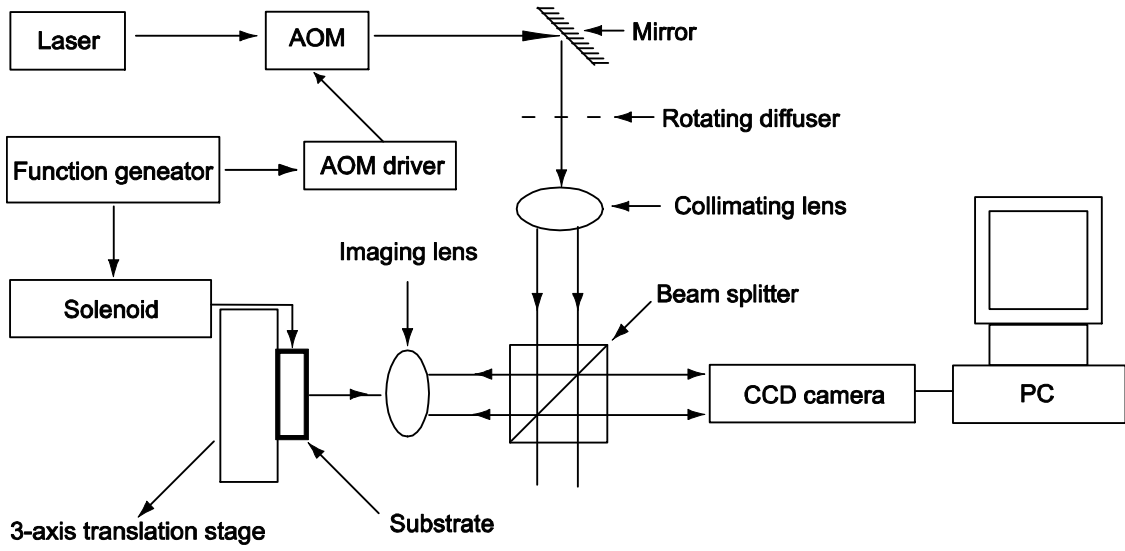
Fig. 1 Measurement setup for MEMS in-plane vibration analysis.
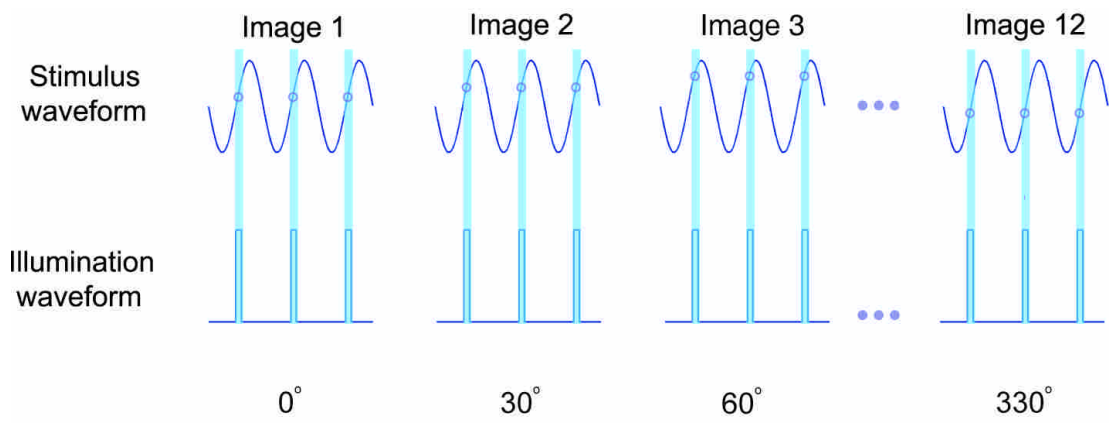
Fig. 2 Stroboscopic generator timing diagram.
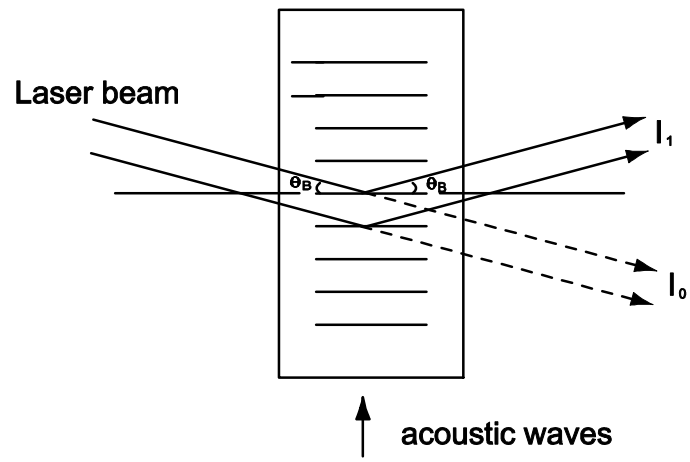
Fig. 3 Bragg regime.
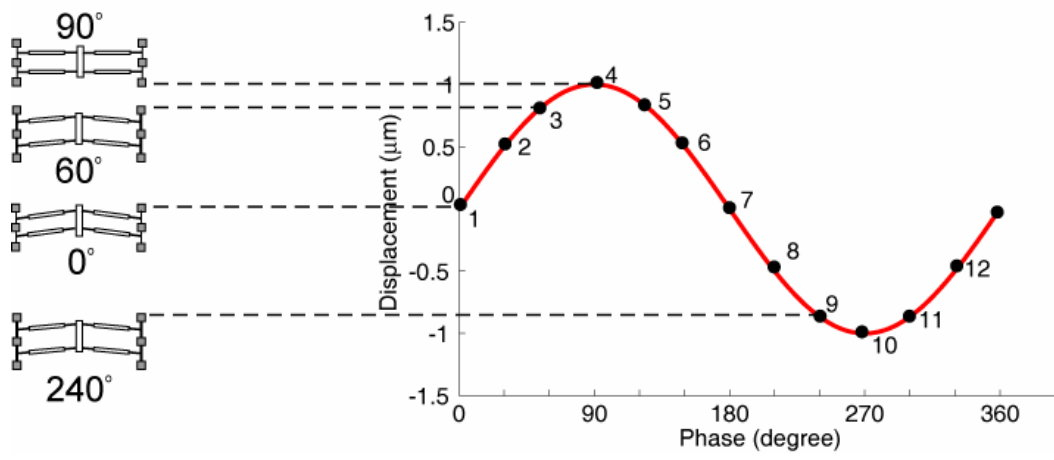
Fig. 4 Schematic of microstructure positions and the corresponding wave form motion.
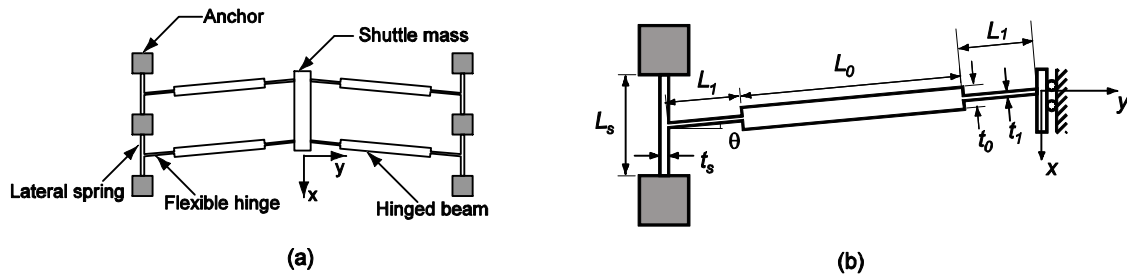
Fig. 5 (a) A schematic of a microstructure. (b) A schematic of a quarter model.

(a) Ti deposition

(b) Coat & pattern photoresist

(c) Ti wet etching

(d) Cu deposition

(e) Strip photoresist

(f) Coat & pattern photoresist

(g) Electroplate Cu

(h) Strip photoresist

(i) Coat & Pattern photoresist

(j) Electroplate Ni-Co

(k) Strip photoresist

(l) Cu wet etching

Glass   Ti   Photoresist   Cu   Ni-Co
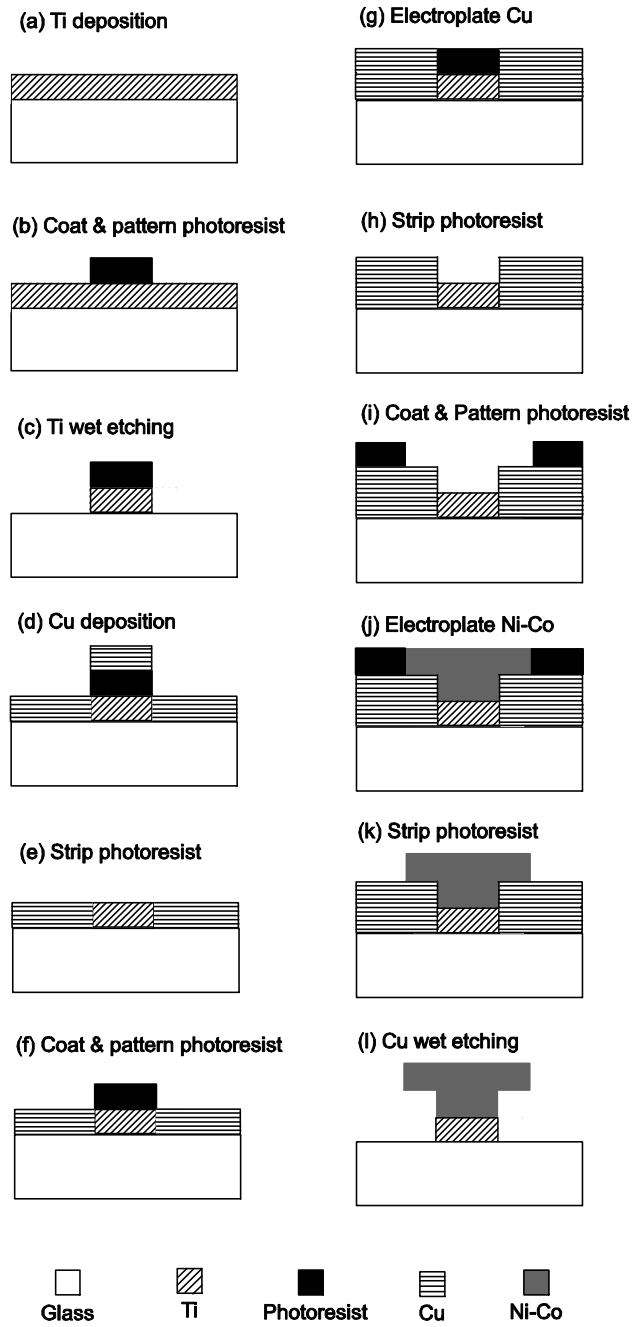
Fig. 6 Fabrication steps.

24
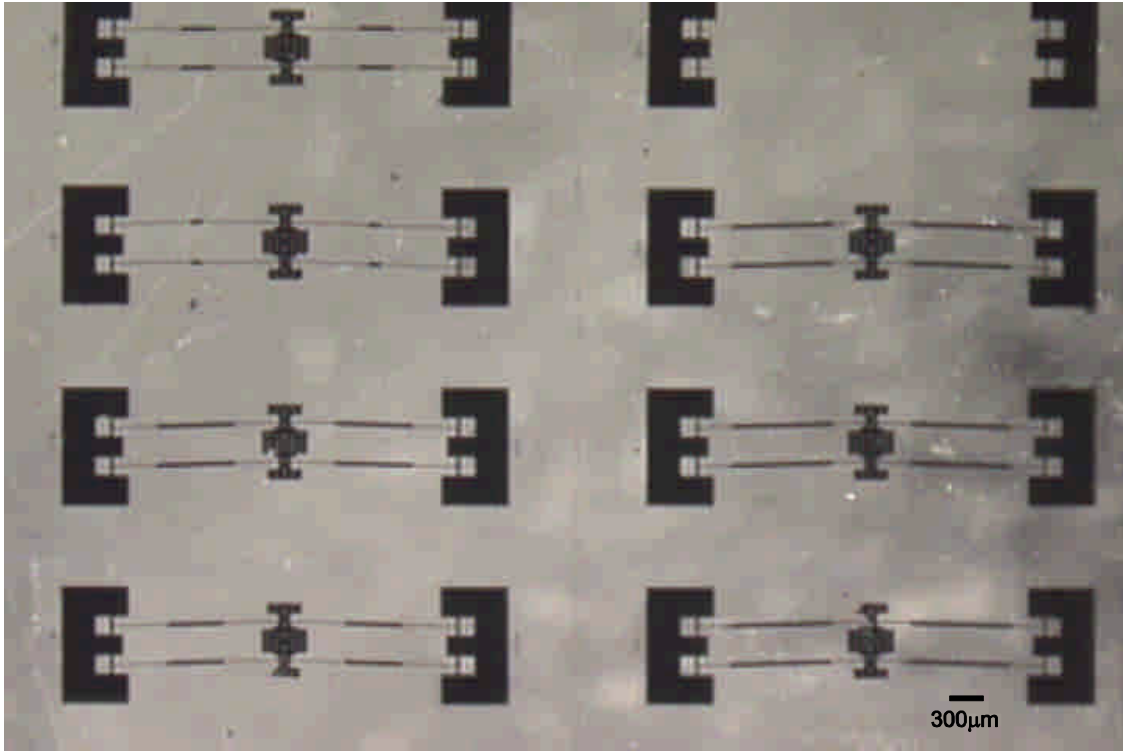
Fig. 7 An array of fabricated devices.
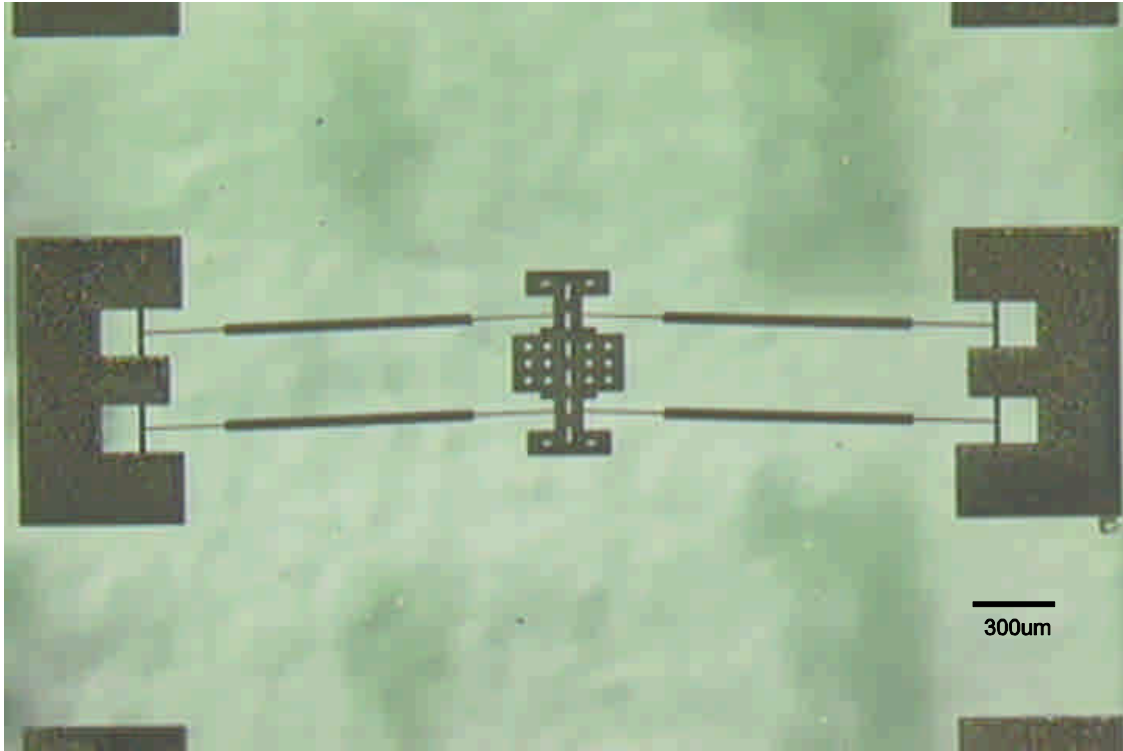
Fig. 8 An OM photo of a fabricated device.
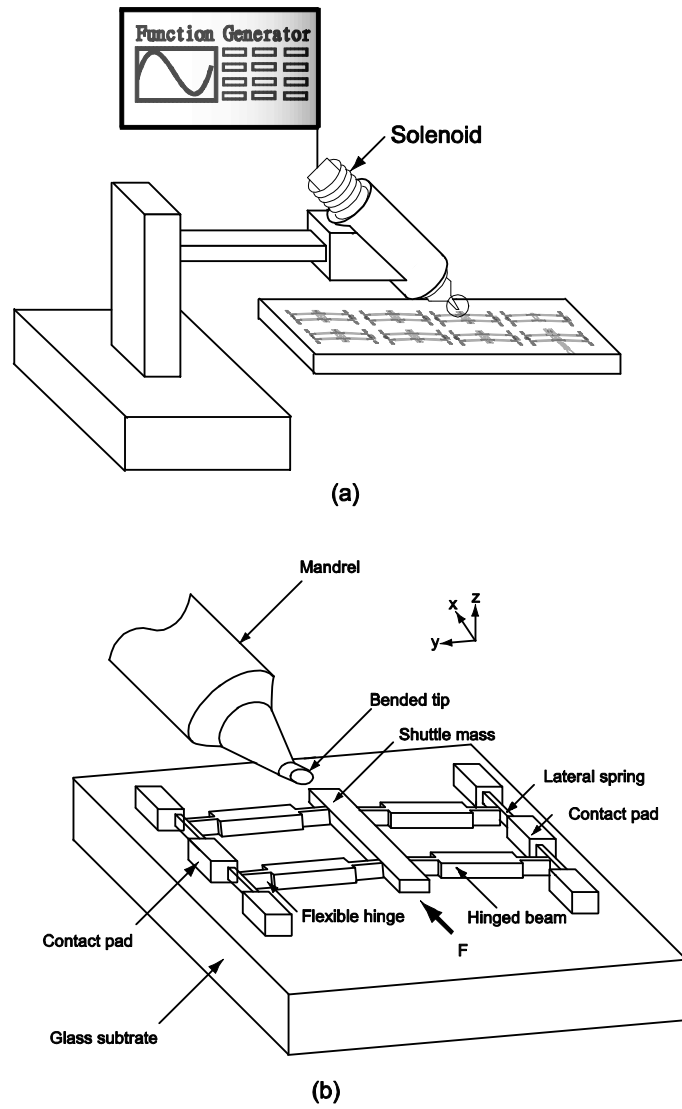
Fig. 9 (a) A schematic of the experimental setup. (b) A close-up view of the mandrel tip and the microstructure.
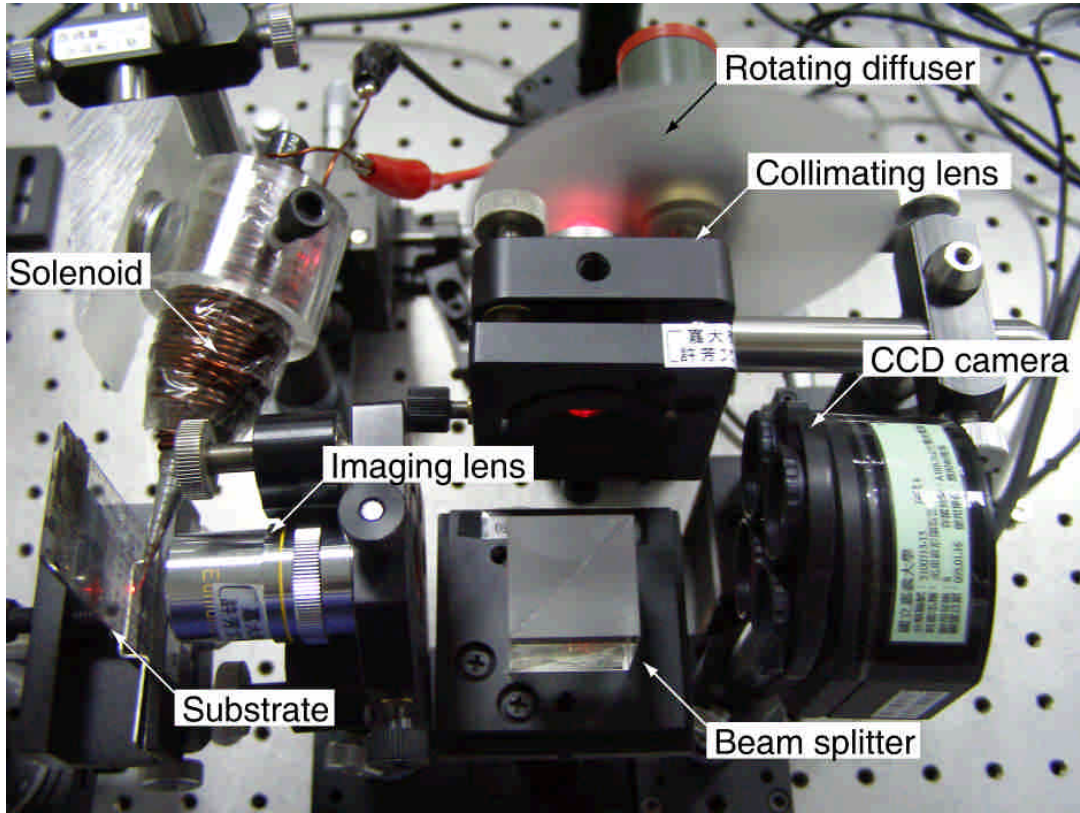
Fig. 10 Photo of the experimental apparatus and the optical measurement setup.

Fig. 11 Images of the twelve phases.
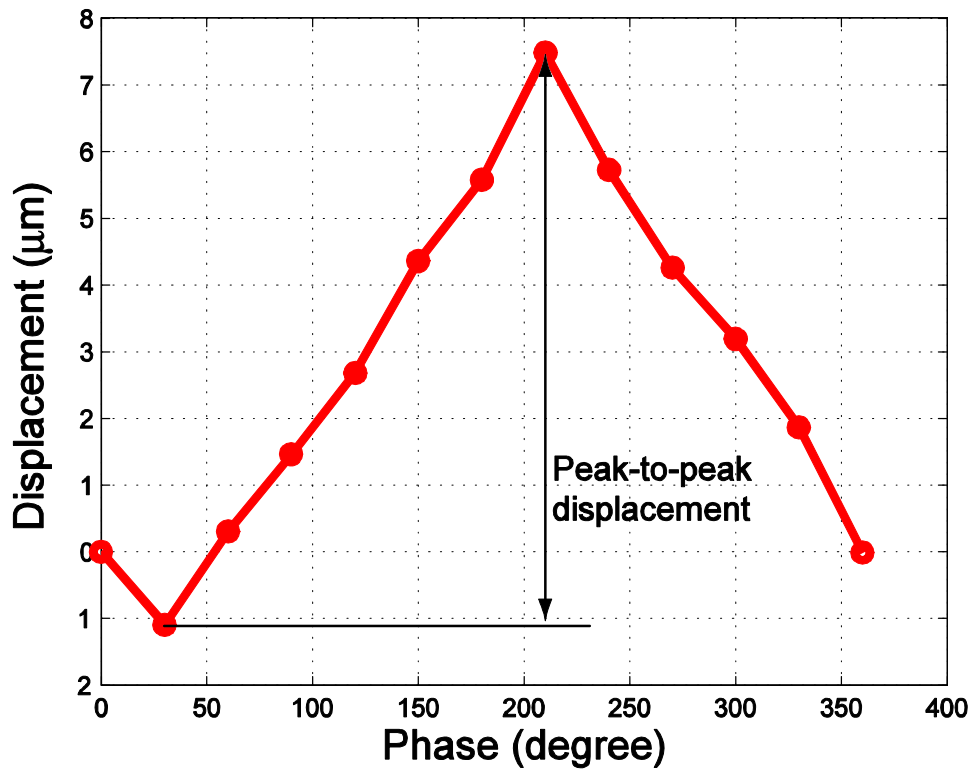
Fig. 12 Displacement as a function of the phases.
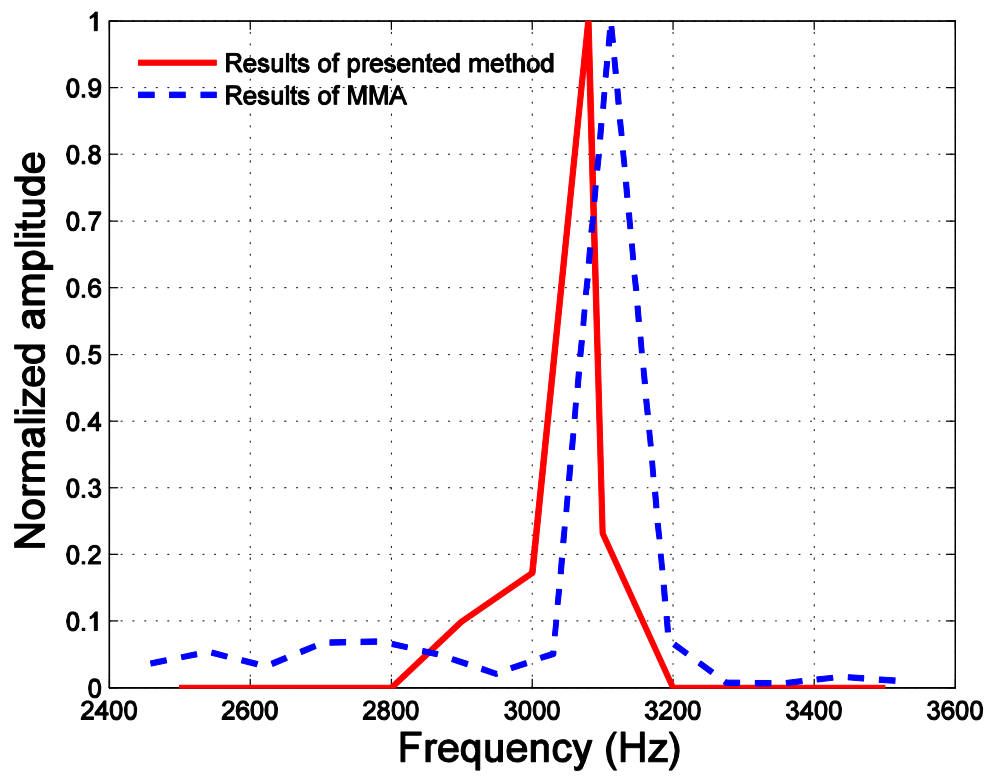
Fig. 13 Harmonic response of the device A.
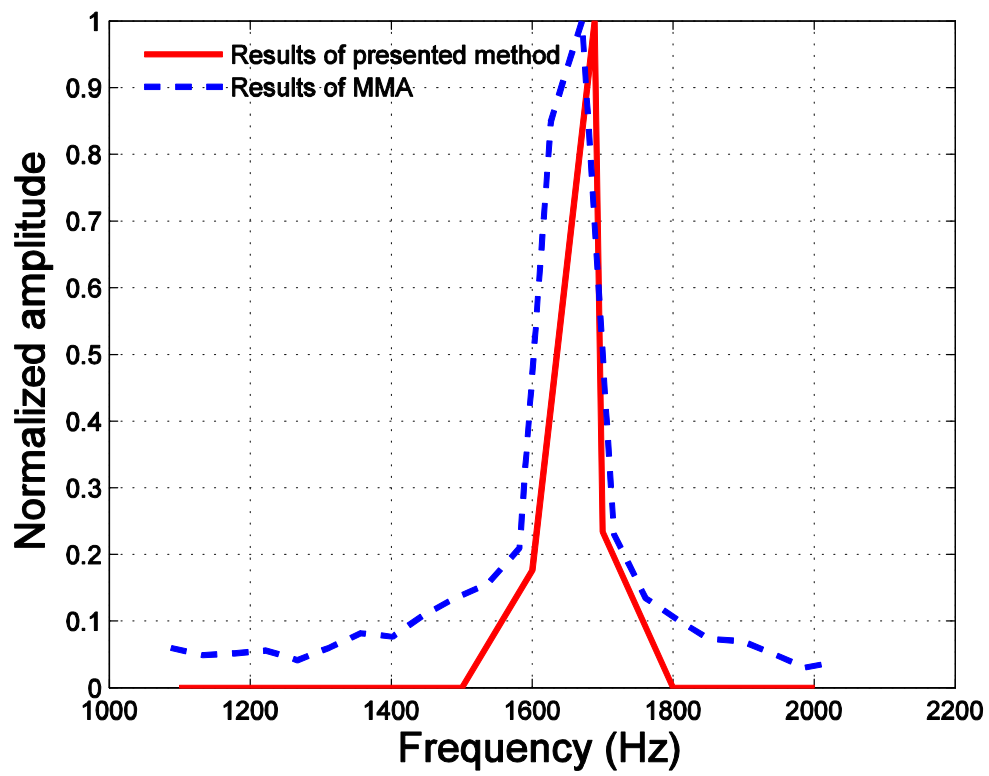
Fig. 14 Harmonic response of the device B.
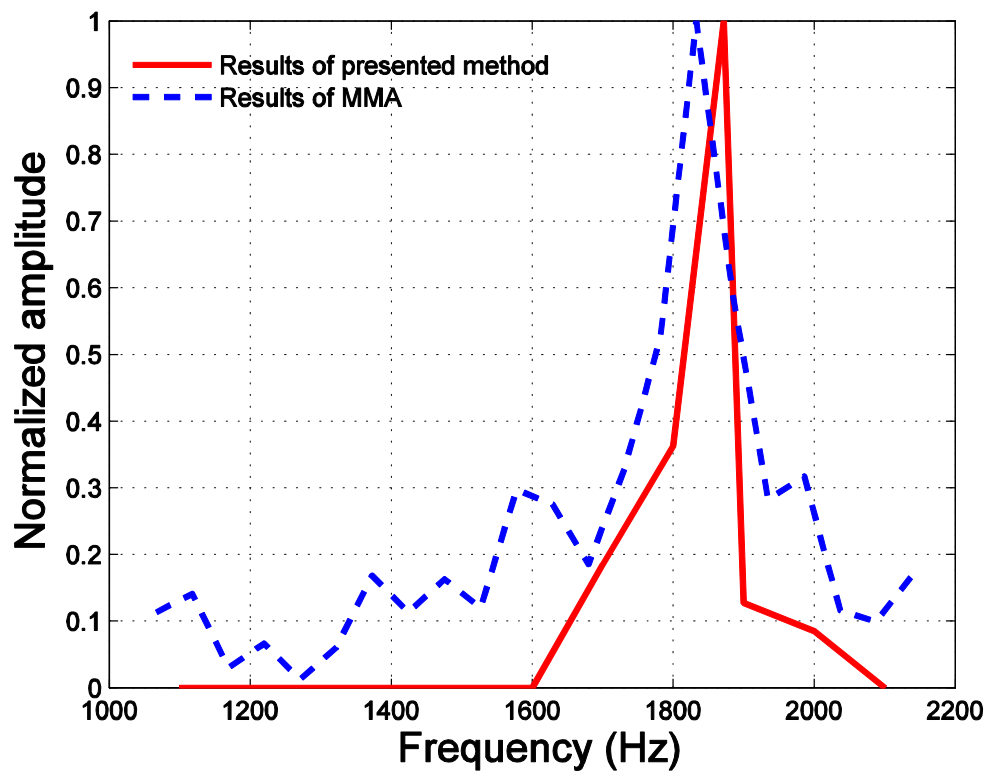
Fig. 15 Harmonic response of the device C.